

# Effect of hatch distance on $\text{CuSn}_{10}$ specimens by selective laser melting

## Abstract

Selective laser melting (SLM) is one of promising additive manufacturing methods, especially for precision parts. Its application in copper alloys is of significance. However, there is rare research achievements about the effect of fabrication parameters on the microstructure and quality of copper alloy parts. In this paper, tin bronze ( $\text{CuSn}_{10}$ ) bars were fabricated with different hatch distance from 0.06mm to 0.1mm and different scanning speed from 198mm/s to 330mm/s, but same area laser energy density. Porosity is mainly dependent on hatch distance instead of scanning speed. The porosity decreases with the decrease of hatch distance. Their microstructure was rose like fine grain cluster growing from melt pool border to pool center, in which fine columnar grain is about  $5\mu\text{m}\times 20\mu\text{m}$  and equi-axed grains is about  $3.5\mu\text{m}$  in diameter. The formed specimens achieved high hardness (78.2HRB) at hatch distance 0.06mm. Fine microstructure leads to the improvement of mechanical properties.

**Keywords:** selective laser melting,  $\text{Cu Sn}_{10}$  bronze alloy, laser energy density, hatch distance, microstructure, hardness

Volume 3 Issue 2 - 2019

Jinwu Kang,<sup>1</sup> Xiang Wang,<sup>1</sup> Chengyang Deng,<sup>1</sup> Yunlong Feng,<sup>1</sup> Tao Feng,<sup>2</sup> Jihao Y.<sup>1,2</sup> Pengyue WU<sup>2</sup>

<sup>1</sup>Tsinghua University, China

<sup>2</sup>Beijing e-Plus 3D Tech.Co. Ltd, China

**Correspondence:** Jinwu Kang, School of Materials Science and Engineering, Key Laboratory for Advanced Materials Processing Technology, Tsinghua University, Beijing 100084, China, Email kangw@tsinghua.edu.cn

**Received:** March 31, 2019 | **Published:** April 08, 2019

## Introduction

Selective laser melting (SLM) is one of promising additive manufacturing methods, especially for precision parts. It can produce complicated three-dimensional shapes in a layer by-layer style. It has been mainly applied into titanium alloys, nickel alloys and steels.<sup>1-3</sup> Tin bronze is widely used as bearing materials for its good friction and wear behaviors. Powders metallurgy (PM), and mechanical ball milling (MBM), and casting are usually used for  $\text{CuSn}_{10}$  powder sintering.<sup>4-8</sup> The porosity and geometry precision are the most concern problems. Additive manufacturing provides a new way to make tin bronze parts. However, the physical properties of copper are different from titanium, nickel alloys and steels, therefore, it is necessary to investigate the principles of selective laser sintering of tin bronze powder. The main parameters of SLM are laser power, scanning speed, layer thickness and hatch distance. Scudino et al.,<sup>9</sup> achieved far better mechanical properties of  $\text{CuSn}_{10}$  specimens by SLM corresponding to as-cast properties. Deng et al.,<sup>10</sup> studied the effect of laser energy density on the microstructure, mechanical properties of Tin bronze parts by SLM and found the laser energy density is the main factor for porosity formation and the mechanical properties. In this paper, The SLM of tin bronze ( $\text{CuSn}_{10}$ ) powder was performed with same laser energy density to investigate the effect of scanning speed and hatch

distance on microstructure and mechanical properties.

## Experiment

A typical Tin bronze alloy  $\text{CuSn}_{10}$  with 90% Cu and 10% Sn is selected for the selective laser melting process. The powder is in the range of 20-50 $\mu\text{m}$ . Bar samples of 20mm $\times$ 20mm $\times$ 45mm were fabricated using the 3D printer EP-M100T (manufactured by Beijing e-Plus 3D Tech. Co. Ltd.). The fabrication parameters are listed in Table 1. Three specimens were produced by different scanning speeds and different hatch distances, but same laser energy density (laser energy divided by hatch distance and scanning speed). The fabrication chamber was filled with argon atmosphere, and the content of oxygen was below 100ppm. The base plate was at room temperature. During the fabrication process, snake scanning routes were adopted and the scanning direction was rotated 60o corresponding to the previous layer, as shown in Figure 1A. The formed bars, as shown in Figure 1B, were removed from the base plate, and then specimens were cut from them for density measurement, hardness test and microstructure observation. The microstructure of the horizontal plane of these specimens were characterized by using a Keyence VHX-6000 digital microscope. The density of the formed specimens was determined by Archimedes method. Hardness was measured by HR-150A Sclerometer.

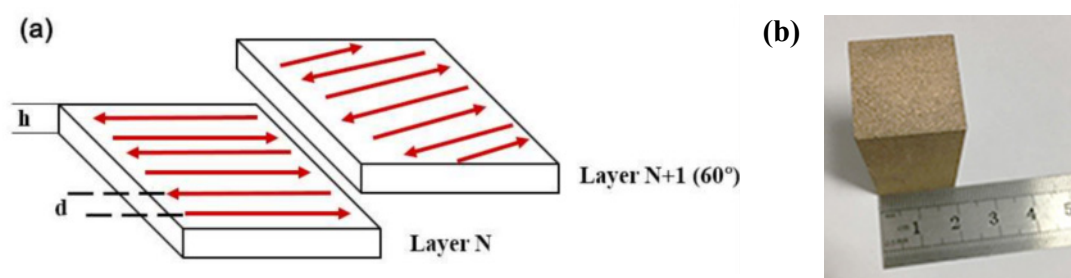


**Figure 1** Laser scanning strategy (A) and a fabricated specimen.

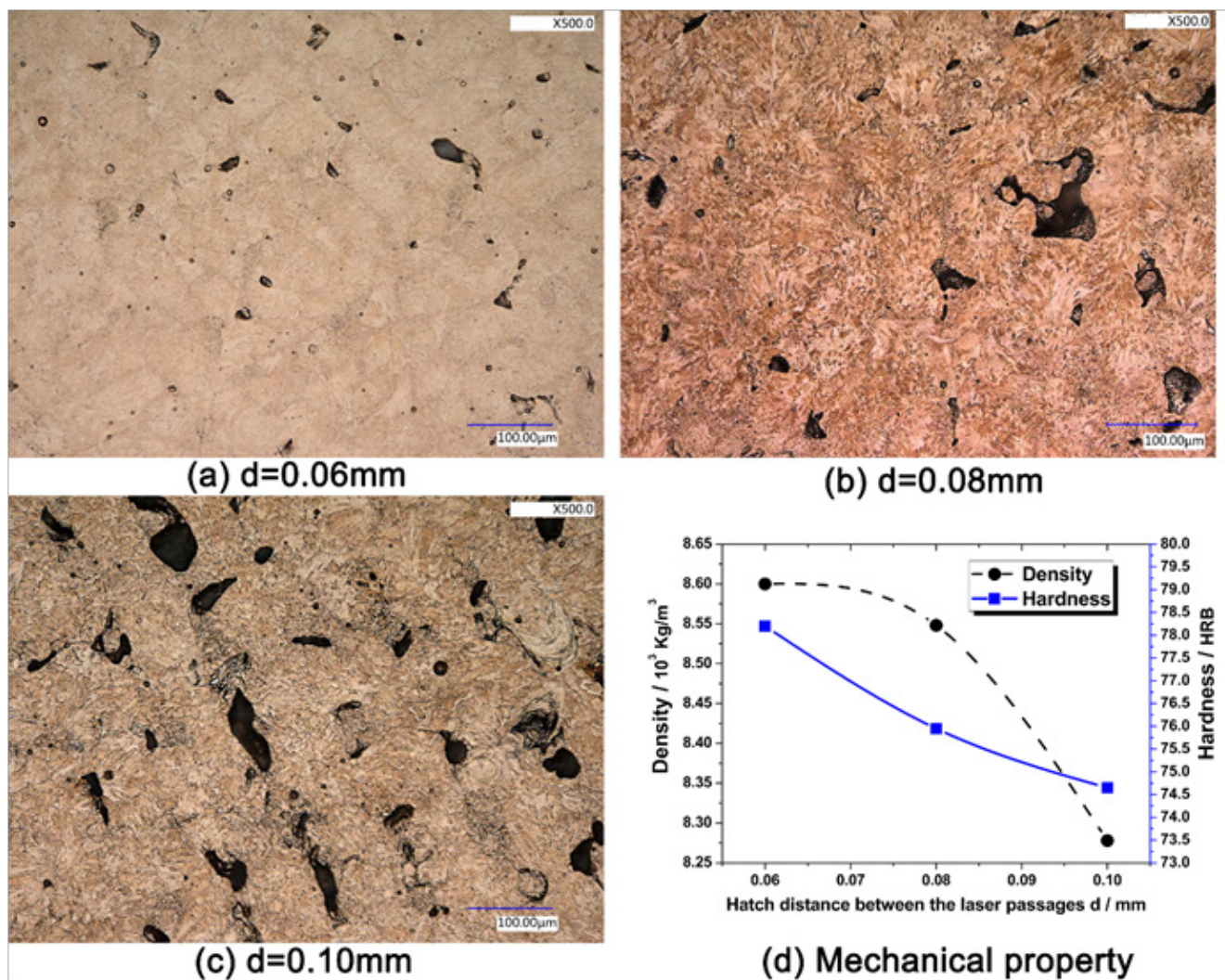
**Table 1** Experimental parameters

| Specimen | Hatch distance /mm | Scanning Speed mm/s | Layer thickness /mm | Laser Power /W | Laser energy density /J/mm <sup>2</sup> |
|----------|--------------------|---------------------|---------------------|----------------|---|
| 1        | 0.06               | 330                 | 0.02                | 95             | 240                                     |
| 2        | 0.08               | 247                 | 0.02                | 95             | 240                                     |
| 3        | 0.10               | 198                 | 0.02                | 95             | 240                                     |

## Results and discussion

The effect of hatch distance on the microstructure and mechanical property of the formed specimens is shown in Figure 2. It can be seen there are number and size of porosities in these specimens, and they increase with the increase of hatch distance. These porosities locate at the border of tracks. The size of porosities in the specimen of 0.06mm is around 10 $\mu$ m. As the hatch distance increases to 0.1mm, the profile of each track is very clear with poor overlapping with adjacent tracks, resulting into strips of porosities around 100 $\mu$ m long and 20 $\mu$ m wide. For all the three conditions, there is only uniformly distributed  $\alpha$ -Cu phase, rose-like fine grain cluster including columnar grains of about 5 $\mu$ m $\times$ 20 $\mu$ m and equi-axed grains of 3.5 $\mu$ m in diameter dispersed

among them grows from the border of melt pool to the moving direction, as shown in Figure 3. Deng et al. found that the mechanical properties increase with the increase of laser energy density in the range of 210-220 J/mm<sup>2</sup> with fixed hatch distance 0.06mm.<sup>11</sup> Here, under the same laser energy condition 240 J/mm<sup>2</sup>, although the scanning speed of specimen #3 is less than that of the specimen #1, but the porosity increases, i.e., the microstructure is mainly dependent on the hatch distance for the hatch distance in the range of 0.06-0.1mm. The density and hardness decrease with the increase of hatch distance, as shown in Figure 2D. The highest density and hardness of reaches 8.60kg/m<sup>3</sup> and 78.2HRB, respectively for specimen #1. The hardness is far higher than that of the as-cast condition. The reason is the fine grains in the as-print condition.

**Figure 2** Microstructure, density and hardness s at different hatch distance.

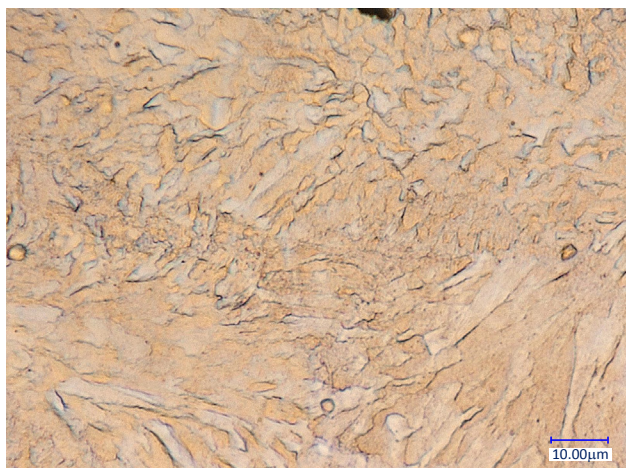


**Figure 3** Microstructure ( $\times 3000$ ) of #1 at hatch distance 0.06mm.

### Conclusion

Tin bronze (CuSn<sub>10</sub>) bars were fabricated with different hatch distance from 0.06mm to 0.1mm and different scanning speed from 198mm/s to 330mm/s, but same area laser energy density. The effect of hatch distance is greater than scanning speed. The porosity decreases with the decrease of hatch distance. Their microstructure was rose like  $\alpha$ -Cu e fine grain cluster growing to melt pool border to pool center. The fine columnar grain is about  $5\mu\text{m} \times 20\mu\text{m}$  and equi-axed grains is about  $3.5\mu\text{m}$  in diameter. The formed specimens achieved high hardness (79HRB) at hatch distance 0.06mm. The fine microstructure leads to the improvement of mechanical properties.

### Acknowledgments

This research study was funded by the National Science and Technology Major Project of the Ministry of Science and Technology of China under Project No. 2016YFB1100703.

### Conflicts of interest

Authors declare that there is no conflict of interest.

### References

1. Deb Roy T, Wei HL, Zuback JS, et al. Additive manufacturing of metallic components – Process, structure and properties. *Progress in Materials Science*. 2018;92:112–224.
2. Kn Amato, Gaytan SM, Murr LE, et al. Microstructures and mechanical behavior of Inconel 718 fabricated by selective laser melting. *Acta Mater*. 2012;60:2229–2239.
3. Jinliang Zhang, Bo Song, Qingsong Wei, et al. A review of selective laser melting of aluminum alloys: Processing, microstructure, property and developing trends. *Journal of Materials Science & Technology*. 2019;35(2):270–284.
4. Canakci A, Varol T, Cuvalci H, et al. Synthesis of novel CuSn<sub>10</sub>-graphite nanocomposite powders by mechanical alloying. *Micro Nano Lett*. 2014;9:109–112.
5. Widyastuti, Vicko GA, Ardhyanta H, et al. Study of Frangible Cu-Sn Composite by Powder Metallurgy Method. *Adv Mater Res*. 2015;1112:497–501.
6. Li T, Yi D, Hu J, et al. Surface modification of h-BN and its influence on the mechanical properties of CuSn<sub>10</sub>/h-BN composites. *J Alloys Compd*. 2017;723:345–353.
7. Dong XJ, Wang LM, Zhang JH, et al. Influence of morphology of different partially alloyed CuSn10 powders on the sintering character self-lubricated bearings. *Powder Metall*. 2010;20:28–32.
8. Afshari E, Ghambari M, Abdolmalek H. Production of CuSn<sub>10</sub> bronze powder from machining chips using jet milling. *Int J Adv Manuf Technol*. 2017;92:663–672.
9. Scudino S, Unterdörfer C, Prashanth KG, et al. Additive manufacturing of Cu–10Sn bronze. *Mater Lett*. 2015;156:202–204.
10. Chengyang Deng, Jinwu Kang, Tao Feng, et al. Study on the Selective Laser Melting of CuSn<sub>10</sub> Powder. *Materials*. 2018;11: 614–620.